

Evidence for superconductivity above 260 K in lanthanum superhydride at megabar pressures

Maddury Somayazulu^{1,*}, Muhtar Ahart¹, Ajay K Mishra², Zachary M. Geballe², Maria Baldini²,
Yue Meng³, Viktor V. Struzhkin², and Russell J. Hemley^{1,*}

¹*Institute for Materials Science and Department of Civil and Environmental Engineering,
The George Washington University, Washington DC 20052, USA*

²*Geophysical Laboratory, Carnegie Institution of Washington, Washington DC 20015, USA*

³*HPCAT, X-ray Science Division, Argonne National Laboratory, Argonne IL 60439, USA*

Recent predictions and experimental observations of high T_c superconductivity in hydrogen-rich materials at very high pressures are driving the search for superconductivity in the vicinity of room temperature. We have developed a novel preparation technique that is optimally suited for megabar pressure syntheses of superhydrides using pulsed laser heating while maintaining the integrity of sample-probe contacts for electrical transport measurements to 200 GPa. We detail the synthesis and characterization, including four-probe electrical transport measurements, of lanthanum superhydride samples that display a significant drop in resistivity on cooling beginning around 260 K and pressures of 190 GPa. Additional measurements on two additional samples synthesized the same way show resistance drops beginning as high as 280 K at these pressures. The drop in resistance at these high temperatures is not observed in control experiments on pure La as well as in partially transformed samples at these pressures, and x-ray diffraction as a function of temperature on the superhydride reveal no structural changes on cooling. We infer that the resistance drop is a signature of the predicted superconductivity in LaH₁₀ near room temperature, in good agreement with density functional structure search and BCS theory calculations.

^{*}zulu58@gwu.edu, rhemley@gwu.edu

The search for superconducting metallic hydrogen at very high pressures has long been viewed as a key problem in physics [1,2]. The prediction of very high (e.g., room temperature) T_c superconductivity in hydrogen-rich materials [3] has opened new possibilities for realizing high critical temperatures but at experimentally accessible pressures (i.e., below 300 GPa) where samples can be characterized with currently available tools. Following the discovery of novel compound formation in the S-H system at modest pressures [4], theoretical calculations have predicted that this material would transform to a superconductor with $T_c = 191\text{-}204$ K at 200 GPa [5,6]. The high critical temperature of 203 K at 150 GPa in samples formed by compression of H_2S was subsequently confirmed [7,8], with x-ray measurements consistent with cubic H_3S as the superconducting phase [9].

Given that the higher hydrogen content in many simple hydride materials is predicted to give still higher T_c values [3], we have extended our studies to higher hydrides, the so-called superhydrides, XH_n with $n > 6$. Systematic theoretical structure searching in the La-H and Y-H systems reveals numerous hydrogen-rich compounds with T_c in the neighborhood of room temperature (above 270 K) [10] (see also Ref. [11]). Of these superhydrides, LaH_{10} and YH_{10} are predicted to have a novel clathrate-type structure with 32 hydrogen atoms surrounding each La or Y atom. These phases are predicted to exhibit strong electron-phonon coupling related to the phonon modes associated with the stretching of H-H bonds within the cages. Both are predicted to have superconducting temperatures near room temperature, i.e., near 270 K at 210 GPa for LaH_{10} and 300 K at 250 GPa in YH_{10} . The superhydride phases consist of an atomic hydrogen sublattice with H-H distances of ~ 1.1 Å, which are close to the predicted values for solid atomic metallic hydrogen at these pressures [12]; for a thorough recent review of the field, see Ref. [13].

Recently, our group successfully synthesized a series of superhydrides in the La-H system up to 200 GPa pressures. Specifically, we reported x-ray diffraction and optical studies demonstrating that the lanthanum superhydrides can be synthesized with La atoms having an fcc lattice at 170 GPa upon heating to ~ 1000 K [14]. The heavy atom sublattice and equation of state are close to those of the predicted cubic metallic phase of LaH_{10} . Experimental and theoretical constraints on the hydrogen content give a stoichiometry of $\text{LaH}_{10\pm x}$, where $x < 1$. On decompression, the fcc-based structure undergoes a rhombohedral distortion of the La sublattice, to form a structure that has subsequently been predicted to also have a high T_c [12]. Here we report the use of a novel synthesis route for megabar pressure syntheses of such superhydrides

using pulsed laser heating and ammonia borane as the hydrogen source. We detail the synthesis and characterization of several samples of the material using x-ray diffraction and electrical resistance measurements at 180-200 GPa. The transport measurements reveal a clear drop in resistivity on cooling at 260 K using four-probe measurements and as high as 280 K in other experiments. We infer that the resistance drop observed in these samples is a signature of nearly room-temperature superconductivity predicted for LaH₁₀.

Samples were prepared using a multi-step process with various piston cylinder-type diamond anvil cells, Composite gaskets consisting of a tungsten outer annulus and a cubic boron nitride epoxy mixture (cBN) insert were employed to contain the sample at megabar pressures while isolating the electrical leads. Four platinum probes were sputtered onto the piston diamond (typically 1-2 μm thick) and connected to the external wires using a combination of 25 μm thick platinum ‘shoes’ and strain relieving copper bronze ‘springs’ [15]. The use of double beveled anvils allowed us to reach the required synthesis pressures and maintain the integrity of the electrical leads. Typically, we used 1/3 carat anvils with a 60 μm central culet beveled to 250 μm at 9° and to 450 μm at 8°.

While it is possible to load a mixture of La and H₂ into such a gasket assembly as in our previous work [14], we found that maintaining a good contact between the synthesized sample and electrodes is not guaranteed. To overcome this problem, we used ammonia borane (NH₃BH₃, AB) as the hydrogen source. When completely dehydrogenated, one mole of AB yields three moles of H₂ plus insulating hBN, the latter serving both as a solid pressure medium and support holding the hydride sample firmly against the electrical contacts (Fig. 1). Although there is limited experimental data on the decomposition reaction kinetics of AB or related compounds above 50 GPa, our extensive earlier studies of the *P-T* dependence of dehydrogenation in AB (and related compounds by other groups) under pressure indicate both release of H₂, and no subsequent uptake of H₂ after release, at high pressures [16-18]. In addition, reports of catalytic dehydrogenation of AB presents the possibility of enhanced chemical activity at the La-AB interface [19].

In a typical run, a 2 μm thick sample of La was sandwiched between the electrodes and AB (typically 5-8 μm thick) in a cBN sample chamber about 40 μm in diameter. When pressure was increased, the rapid compression of the softer AB caused the cBN sample chamber to thin

rapidly. We found that an initial cBN gasket thickness less than 15 μm guaranteed no implosion of the cBN gasket, which would in turn compromise the electrodes. Both La and AB were loaded in a glovebox in Ar environment with very low O₂ and H₂O content (<0.1 ppm and <1 ppm, respectively). We also found that no chemical damage to the La sample occurred if it was loaded outside the glovebox within 30 mins of being removed, as this was needed to use a micromanipulator outside the glovebox to position the sample precisely on the piston diamond. The cell was clamped inside the glovebox and pressure typically raised to about 60 GPa.

After loading, synchrotron x-ray diffraction of the La-AB mixture was measured on the 16-ID-B beamline at Sector 16, HPCAT at the Advanced Photon Source, Argonne National Laboratory. Typically, a 5 x 5 μm focused x-ray beam at 0.4046 Å was rastered across the sample. This served as both the check on the chemical integrity of the sample as well as determining the spatial extent over which laser heating needed to be performed for synthesis. A typical data set showed no evidence for reactions taking place during rapid compression without heating. Further, no appreciable peak broadening occurred on compression, indicating that AB served as a reasonably quasihydrostatic pressure medium. Pressure was determined using x-ray diffraction from a gold pressure marker [20] and from the Raman shift of the diamond anvil tip with a 660 nm laser source [21]. The observed compression of the La sample determined by x-ray diffraction was found to coincide with a control run using Ne as a pressure medium [14], further confirming that the AB remained quasihydrostatic over these conditions.

These complex heating experiments were possible due to a versatile laser heating system that was conditioned for our experiments [22]. *In-situ* laser heating of the sample with a Nd-YLF laser was performed at pressures above 185 GPa, since this was observed to be the lowest pressure for which LaH_{10±x} is both synthesized and remains stable [14]. Only single-sided laser heating was conducted since the synthesis is expected to proceed from the La-AB interface, and this was the side that is buffered from both the diamond and the electrodes (Fig. 1). The pulse width of the heating laser was held at 5 ms while increasing power. In all runs, we observed very good coupling and subsequent sharpening of diffraction peaks followed by partial transformation of the sample to cubic LaH_{10±x} when temperatures were above 1200 K. Above 2000 K, we observed a new diffraction peaks, including those indicating a monocline unit cell similar to that reported for Mg(BH₂)₂ [23]. To complete the transformation, we needed to maintain sample

temperatures below 1800 K. This was achieved by varying the combination of laser power and pulse width of the heating laser. Typically, we found that a 300 ms pulse resulted in better transformation, better coverage and the lowest damage threshold. The laser spot size was kept to roughly 30 μm to cover the sample while chilled water was circulated around the cell to minimize movement due to thermal expansion of assembly components. This aspect of the system was crucial since movement of the cell would result in changes in laser alignment and/or laser spot size that could damage the electrodes as well. The sample was then rastered in the x-ray beam following the laser heating to confirm complete transformation. Typically, we found that the region in contact with the electrodes could be partially transformed [15], which is plausible since the electrodes would act as an additional heat sink with which the sample has thermal contact. We also performed a check on the two-probe resistance between the four electrodes between heating cycles to ensure that the electrodes were not damaged. The cells were then introduced into a flow-type cryostat (i.e., off-line from the x-ray measurements), and the leads connected to a function generator and lock-in amplifier for the electrical conductivity measurements [24]. The pressure was monitored from diamond Raman measurements after each cooling and warming cycle. While every effort was made to minimize pressure excursions during cooling cycles (by using opposing load screws), we found that in cells made of stainless steel, pressure increased marginally during the first cooling cycle by at least 10 GPa.

Representative diffraction patterns of three samples are shown in Fig. 2, including a $\text{LaH}_{10\pm x}$ sample that was verified to have the four-probe geometry intact when the pressure was measured to be 188 GPa before cooling (and deviated slightly while cooling). The characteristic diffraction peaks of $\text{LaH}_{10\pm x}$ identified previously from the synthesis using La and H_2 are observed, demonstrating that the superhydride phase can indeed be synthesized from La and AB using the techniques described above. Further, the results presented below show that synthesis can be carried out while maintaining the electrical leads intact (Fig. 1).

Figure 3 shows an example of a resistance measurement on cooling the sample first reported in Ref. [25]. The voltage applied was 330 mV (rms, 1V p-p applied across $\sim 1 \text{ k}\Omega$) at 100 kHz and the drop in resistance was observed to begin at around 275 K and to drop appreciably at 260 K. The resistance remained constant and near zero to at least 150 K. After verifying that the pressure had not increased significantly, we performed a warming cycle where

we observed a reversible change in the resistance of the sample. We observed a dramatic loss of resistivity on cooling. The drop in resistance shown in Fig. 3 was reversible, but the onset changed with cycling. The initial 300 K pressure was 188 GPa [21], but after the first cooling (blue) and warming (red) cycle it increased to 196 GPa. It is normal for the pressure to increase dramatically when cooling with the diamond cell used in this experiment. Figure S2 and S3 show additional measurements (summarized in Table S1) that all show a dramatic loss of resistance beginning between 260 and 280 K at pressures up to 200 GPa [15]. Together with the four-probe measurement data (Fig. 2) the data show confirmatory results. Since the pressure in all cases was measured at room temperature outside of the cryostat, the actual pressure dependence of T_c is somewhat uncertain.

Additional experiments were carried out to address the question of whether the change drop in resistance at 260-280 K in the material is due to a temperature-induced structural change. To test this, as well as to identify other possible structural changes in the samples on thermal cycling, *in situ* x-ray diffraction measurements were performed as a function of temperature after synthesizing $\text{LaH}_{10\pm x}$ under pressure. The x-ray diffraction patterns reveal no structural changes in the sample and indicated changes in pressure of $\Delta P = 0.1$ GPa (Fig. S4) on cycling from 300 K to 150 K.

We now discuss in more detail the electrical conductivity data. We emphasize that the high-temperature phase (i.e., normal state) is a metal. An alternative explanation for the drop in conductivity is temperature-induced, iso-structural electronic transition with a dramatic increase in conductivity in the low temperature phase not associated with superconductivity. However, calculations to date have failed to predict such a transition. We did not attempt to estimate any geometric corrections based on the sample dimensions purely because we recognize that this could be a mixed phase, possibly with varying hydrogen stoichiometry [10]. It is possible that the sample could be consisting of layers of LaH_x starting from $x = 10$ on the laser heated side and $x < 10$ toward the electrodes. In some cases, we also observed a drop in resistance but preceded by a complex, unexpected rise in resistance while cooling [15]. These results can be explained by the variable sample stoichiometry observed in the x-ray diffraction patterns. The diffraction pattern of this particular sample showed the coexistence of $\text{LaH}_{10\pm x}$, unreacted La and some monoclinic $\text{La}(\text{BH}_2)_3$. It is also possible that the drop in resistance signifies a changing network

of superconducting material on thermal cycling. We also acknowledge that the samples could have a complicated toroidal geometry consisting of a central region of $\text{LaH}_{10\pm x}$ with a peripheral ring of untransformed La arising from the need to preserve the electrodes during laser heating and differential thermal heat transport for the sample in contact with the diamond versus that contact with the electrodes. Similarly, we expect that the hysteresis in the characteristic temperature where a dramatic resistance drop is observed could be due to a combination of pressure and geometric effects (see Fig. 3 and Ref. [15]). The increase in pressure also affected the contact resistance as evidenced by a large decrease after the cooling cycle especially in samples that were probed with pseudo-four probe techniques. Also, the complexity of the experiments prevents us from accurately determining the pressure dependence of T_c . However, the four-probe measurements do suggest a decrease in T_c with pressure, in agreement with theory [10]. The drop in resistance in the pseudo-four probe measurements (i.e., $\sim 10\%$) is comparable to what is observed in similar measurements of other superconducting transitions under pressure.

In summary, we report resistance measurements on $\text{LaH}_{10\pm x}$ synthesized at pressures of 180-200 GPa by a pulsed laser technique that preserves the integrity of multi-probe electrical contacts on the sample after synthesis. These experiments remain challenging due to the requirement that the electrical probes not be damaged, and the limited temperature range of the synthesis. Nevertheless, our multiple measurements reveal the signature of a major resistance drop at consistent high temperatures of 260-280 K at 190-200 GPa. The drop in resistance occurs around the same temperature as predicted by BCS calculations for the ideal LaH_{10} structure, although the stability extends to somewhat lower pressure than that originally predicted [10]. Further work is obviously needed, including conductivity measurements using more advanced sample preparation techniques such as nano-lithographic methods for improved measurements of conductivity following high-temperature synthesis. Measurements of the shift in T_c with magnetic field as well as direct measurements of the Meissner effect are also needed. Additional measurements along these lines are in progress, including additional information from optical and infrared spectroscopy. Nevertheless, these measurements reported here provide evidence of conventional superconductivity near room temperature in novel dense hydride materials.

Acknowledgements

We are grateful to H. Liu, I. I. Naumov, R. Hoffman, N. W. Ashcroft, and S. A. Gramsch for their help in many aspects of this work. The authors would like to acknowledge the support of Paul Goldey and honor his memory. This research was supported by EFree, an Energy Frontier Research Center funded by the U.S. Department of Energy (DOE), Office of Science, Office of Basic Energy Sciences, under Award DE-SC0001057. The infrastructure and facilities used were supported by the U.S. DOE/National Nuclear Security Administration (Award DE-NA-0002006, CDAC; and Award DE-NA0001974, HPCAT). The Advanced Photon Source is operated for the DOE Office of Science by Argonne National Laboratory under Contract DE-AC02-06CH11357.

References

- [1] N. W. Ashcroft, Metallic hydrogen - A high-temperature superconductor, *Phys. Rev. Lett.* **21**, 1748 (1968).
- [2] V. L. Ginzburg, What problems of physics and astrophysics seem now to be especially important and interesting (thirty years later, already on the verge of XXI century)?, *Phys. Uspekhi* **42**, 353 (1999).
- [3] N. W. Ashcroft, Hydrogen dominant metallic alloys: high temperature superconductors?, *Phys. Rev. Lett.* **92**, 187002 (2004).
- [4] T. A. Strobel, P. Ganesh, M. Somayazulu, P. R. C. Kent and R. J. Hemley, Novel cooperative interactions and structural ordering in H₂S-H₂, *Phys. Rev. Lett.* **107**, 255503 (2011).
- [5] Y. Li, J. Hao, H. Liu, Y. Li and Y. Ma, The metallization and superconductivity of dense hydrogen sulfide, *J. Chem. Phys.* **140**, 174712 (2014).
- [6] D. Duan, *et al.*, Pressure-induced metallization of dense (H₂S)₂H₂ with high-T_c superconductivity, *Sci. Rep.* **4**, 6968 (2014).
- [7] A. P. Drozdov, M. I. Eremets and I. A. Troyan, Conventional superconductivity at 190 K at high pressures, *arXiv:1412.0460*
- [8] A. P. Drozdov, M. I. Eremets, I. A. Troyan, V. Ksenofontov and S. I. Shylin, Conventional superconductivity at 203 K at high pressures, *Nature* **525**, 73-76 (2015).
- [9] M. Einaga, *et al.*, Crystal structure of the superconducting phase of sulfur hydride, *Nature Phys.* **12**, 835-838 (2016).
- [10] H. Liu, I. I. Naumov, R. Hoffmann, N. W. Ashcroft and R. J. Hemley, Potential high-T_c superconducting lanthanum and yttrium hydrides at high pressure, *Proc. Natl. Acad. Sci. USA* **114**, 6990-6995 (2017).
- [11] F. Peng, Y. Sun, C. J. Pickard, R. J. Needs, Q. Wu and Y. Ma, Hydrogen clathrate structures in rare earth hydrides at high pressures: Possible route to room-temperature superconductivity, *Phys. Rev. Lett.* **119**, 107001 (2017).
- [12] H. Liu, I. I. Naumov, Z. M. Geballe, M. Somayazulu, J. S. Tse and R. J. Hemley, Dynamics and superconductivity in compressed lanthanum superhydride, *submitted*
- [13] T. Bi, N. Zarifi, T. Terpstra and E. Zurek, The search for superconductivity in high pressure hydrides, *arXiv:1806.00163*.
- [14] Z. M. Geballe, *et al.*, Synthesis and stability of lanthanum superhydrides, *Angew. Chem. Inter. Ed.* **57**, 688-692 (2018).
- [15] Supplementary Materials
- [16] R. S. Chellappa, M. Somayazulu, V. V. Struzhkin, T. Autrey and R. J. Hemley, Pressure-induced complexation of NH₃BH₃-H₂, *J. Chem. Phys.* **224515** (2009).
- [17] Y. Song, New perspectives on potential hydrogen storage materials using high pressure, *Phys. Chem. Chem. Phys.* **15**, 14524–14547 (2013).
- [18] R. G. Potter, M. Somayazulu, G. D. Cody and R. J. Hemley, High pressure equilibria of dimethylamine borane, dihydridobis(dimethylamine)boron(III) tetrahydridoborate(III), and hydrogen *J. Phys. Chem. C* **118**, 7280-7287 (2014).
- [19] W.-W. Zhan, Q.-L. Zhu and Q. Xu, Dehydrogenation of ammonia borane by metal nanoparticle catalysts, *ACS Catalysis* **6**, 6892-6905 (2016).

- [20] D. L. Heinz and R. Jeanloz, The equation of state of the gold calibration standard, *J. Appl. Phys.* **55**, 885 (1984).
- [21] Y. Akahama and H. Kawamura, Pressure calibration of diamond anvil Raman gauge to 310 GPa, *J. App. Phys.* **100**, 043516 (2006).
- [22] Y. Meng, G. Shen and H. K. Mao, Double-sided laser heating system at HPCAT for in situ x-ray diffraction at high pressures and high temperatures, *J. Phys. Cond. Matter* **18**, S1097 (2007).
- [23] R. Černý, Y. Filinchuk, H. Hagemann and K. Yvon, Magnesium borohydride: synthesis and crystal structure, *Angew. Chem. Inter. Ed.* **46**, 5765-5767
- [24] L. J. van der Pauw, A method of measuring specific resistivity and Hall effect of discs of arbitrary shape, *Philips Res. Rep.* **13**, 1-9 (1958).
- [25] R. J. Hemley, Progress on hydride, superhydride, and hydrogen superconductors, *International Symposium: Pressure and Superconductivity. Fundacion Ramon Areces - Madrid, Spain, May 21-22* (2018).
- [26] A. Dewaele, P. Loubeyre and M. Mezouar, Equations of state of six metals above 94 GPa, *Phys. Rev. B* **70**, 094112 (2004).
- [27] P. Loubeyre, *et al.*, X-ray diffraction and equation of state of hydrogen at megabar pressure, *Nature* **383**, 702-704 (1996).
- [28] A. G. Gavriliuk, V. V. Struzhkin, I. S. Lyubutin, M. Y. Hu and H. K. Mao, Phase transition with suppression of magnetism in BiFeO₃ at high pressure, *JETP Letters* **82**, 224-227 (2005).

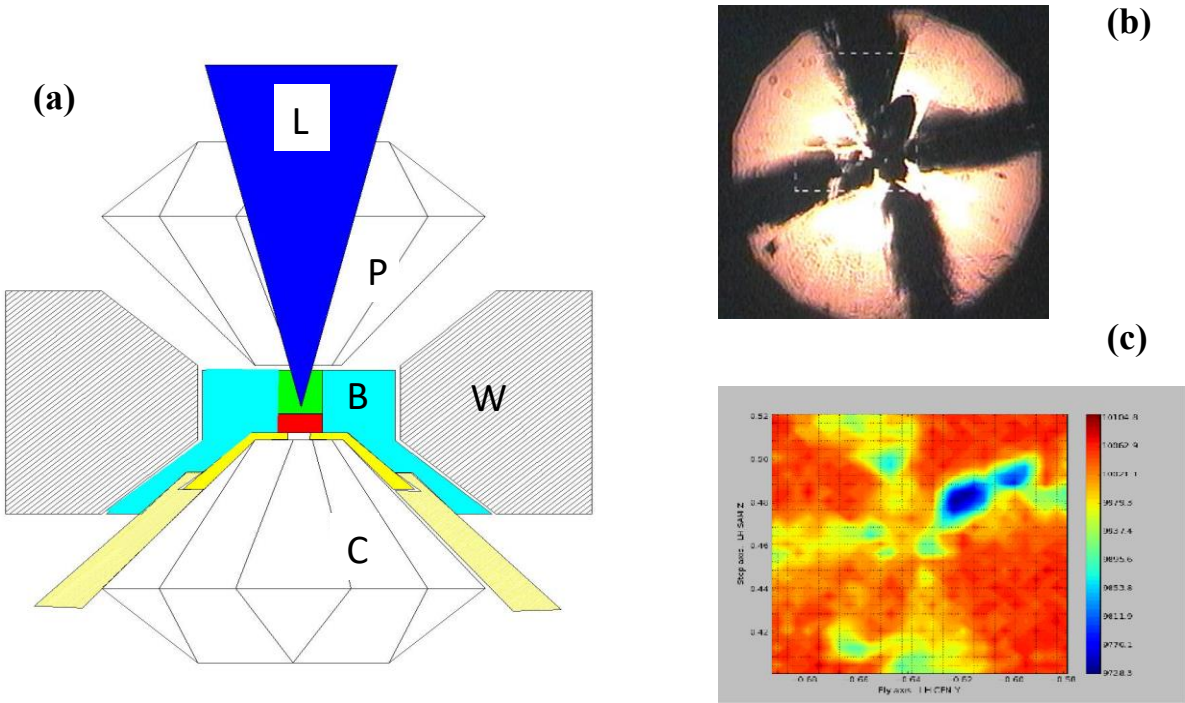


Figure 1. (a) Schematic of the assembly used for synthesis and subsequent conductivity measurements. The sample chamber consists of a tungsten outer gasket (W) with an insulating cBN insert (B). The piston diamond (P) is coated with four $1\text{-}\mu\text{m}$ thick Pt electrodes which are pressure bonded to $25\text{ }\mu\text{m}$ thick Pt electrodes (yellow). The $5\text{ }\mu\text{m}$ thick La sample (red) is placed on the Pt electrodes and packed in with ammonia borane (AB, green). Once the synthesis pressure is reached, the single-sided laser heating (L) is used to initiate the dissociation of AB and synthesis of $\text{LaH}_{10\pm x}$. To achieve optimal packing of AB without compromising the gasket strength, we loaded AB first with the gasket fixed on the cylinder diamond (C). (b) Optical micrograph of the sample at 178 GPa after laser heating. (c) X-ray transmission radiograph of the assembly in a similar orientation, which shows the sample confined to the junction of the four Pt electrodes. The radiograph was reconstructed from contouring the transmitted x-ray intensity ($\lambda = 0.4066\text{ \AA}$, or $E = 30.492\text{ keV}$) on a photodiode behind the sample which was rastered in perpendicular x and y directions in $2\text{ }\mu\text{m}$ steps.

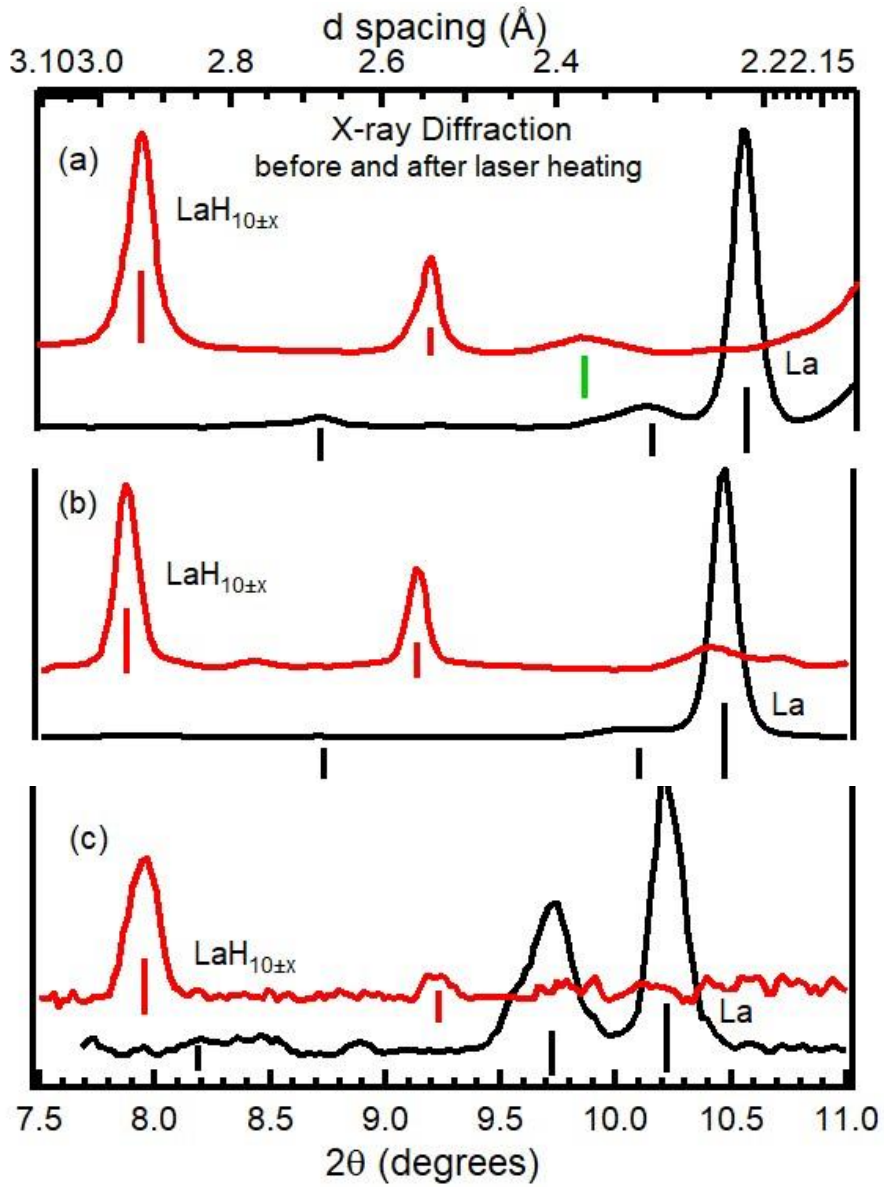


Figure 2. Synchrotron x-ray diffraction patterns obtained from three samples in which $\text{LaH}_{10\pm x}$ was synthesized by laser heating at pressures above 175 GPa. (a) X-ray diffraction following laser heating of a mixture of La and H_2 ; (b) and (c) results obtained following laser heating of La and NH_3BH_3 . The data were obtained from three separate runs with a nominal x-ray spot size of $5 \times 5 \mu\text{m}$. In all three panels, the data shown in black are from the *hR24* phase of La, and the pattern shown in red is from the fcc-based $\text{LaH}_{10\pm x}$ obtained after laser heating above 175 GPa. The sample shown in (c) was nominally $5 \mu\text{m}$ thick and shows a high degree of stress (both in the relative intensities and the broadening of the diffraction peaks of the *hR24* phase). The diffraction peak marked by the green symbol in (a) is residual WH_x which is formed when H_2 is present. This peak is absent in the other two patterns obtained with the insulating cBN gasket.

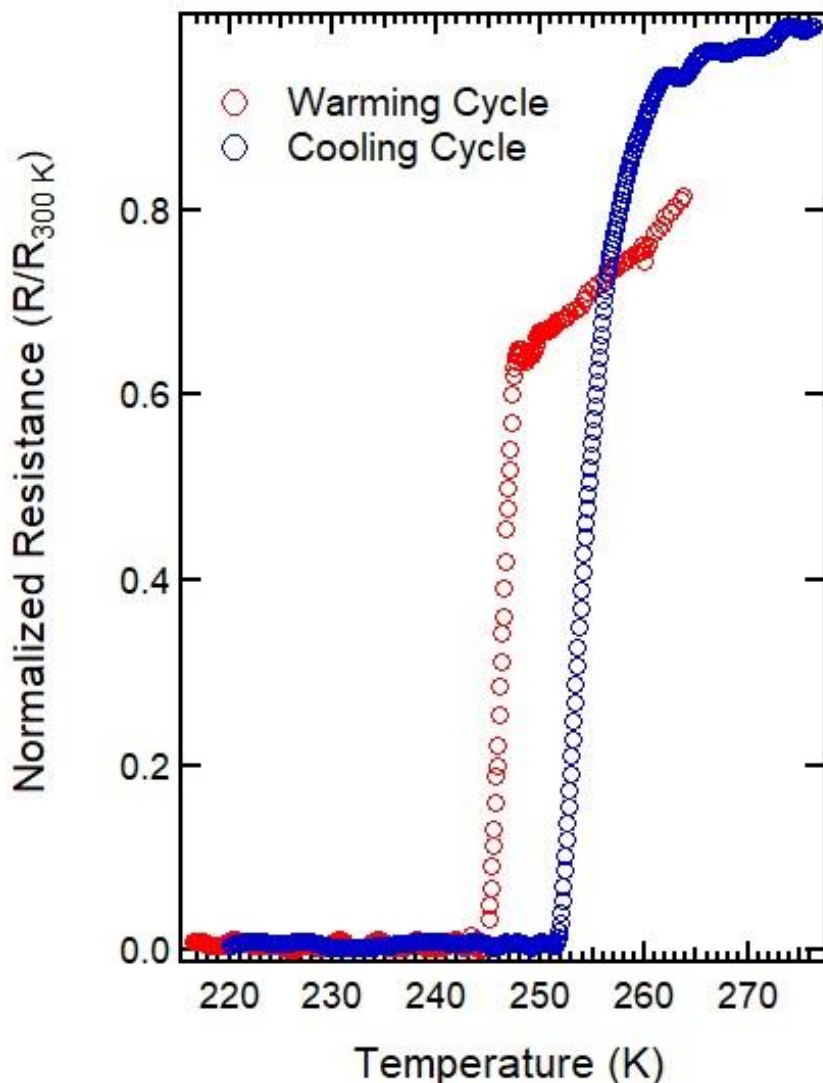


Figure 3. Normalized resistance of the LaH_{10+x} sample characterized by x-ray diffraction and radiography (Figs. 1 and 2) and measured with a four-probe technique. The initial pressure was 188 GPa as determined from the Raman measurements of the anvil diamond edge; the pressure after the first cooling (blue) and warming (red) cycle was found to be 196 GPa. The lowest resistance we could record was approximately $50 \mu\Omega$ after the drop shown in the plot; the 300 K value was $50 \text{ m}\Omega$). These measurements were performed using a EG and G model 5209 lock-in amplifier with nominally 10 mA current at 1 kHz with a typical cooling and warming rate of 1 K/min.

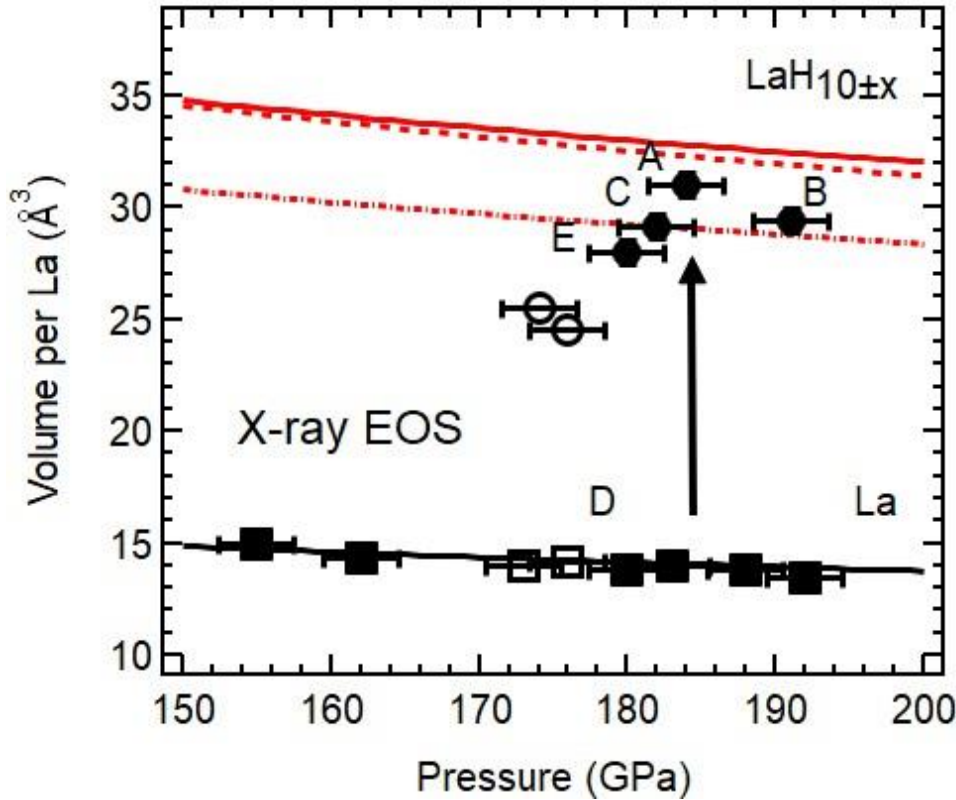


Figure 4. Observed volumes per La before and after the conversion from La to $\text{LaH}_{10\pm x}$ are shown for several samples for which low temperature conductivity measurements have been performed. Several other samples that lost electrical contacts have been excluded. All these samples used NH_3BH_3 as the hydrogen source and were laser heated at pressures higher than 170 GPa (as determined by a combination of diamond Raman [21] and Pt equation of state [26]). The x-ray determined P - V equations of state we reported earlier for $\text{LaH}_{10\pm x}$ and La are shown by the solid lines [14]. The predicted P - V curves for the assemblages La + 5H₂ and La + 4H₂ are plotted as the dashed and dash-dot lines (respectively). The arrow indicates the superhydride synthesis, which is accompanied by conversion of the rhombohedral ($R-3m$) $hR24$ phase of La to cubic ($Fm-3m$) $\text{LaH}_{10\pm x}$ and an increase in the volume per La. Depending on the peak temperature, the heating laser pulse width, the thickness of the La sample (and the gasket thickness which dictates the La to NH_3BH_3 ratio), we synthesize cubic $\text{LaH}_{10\pm x}$. The samples A-C show resistivity drops in comparison to the untransformed sample D that shows a monotonic decrease with temperature. The resistance in the samples denoted by open symbols were also measured and displayed no transitions on cooling (although these two samples in fact had all the four probes intact after synthesis). These volumes were calculated using the reported equations of state for La [14] and molecular H₂ [27]. Samples A, B, and C, which show conductivity drops and E (used in the low temperature x-ray diffraction experiment) have volumes that suggest hydrogen content with x as low as 2 while still maintaining a cubic La. In contrast, samples that did not show any evidence of the conductivity drop between 300 and 80 K lie below the La + 4H₂ line. The synthesis conditions of the samples labeled in the figure are listed in Table S1.

Supplementary Materials

Evidence for superconductivity above 260 K in lanthanum superhydride at megabar pressures

Maddury Somayazulu^{1,*}, Muhtar Ahart¹, Ajay K Mishra², Zachary M. Geballe², Maria Baldini²,
Yue Meng³, Viktor V. Struzhkin², and Russell J. Hemley^{1,*}

¹*Institute for Materials Science and Department of Civil and Environmental Engineering,
The George Washington University, Washington DC 20052, USA*

²*Geophysical Laboratory, Carnegie Institution of Washington, Washington DC 20015, USA*

³*HPCAT, X-ray Science Division, Argonne National Laboratory, Argonne IL 60439, USA*

*zulu58@gwu.edu, rhemley@gwu.edu

We have developed a novel preparation technique that is optimally suited for megabar pressure syntheses of superhydrides using pulsed laser heating while maintaining the integrity of sample-probe contacts for electrical transport measurements to 200 GPa. We report the synthesis and characterization, including four-probe electrical transport measurements, of lanthanum superhydride samples that display a significant drop in resistivity on cooling beginning around 260 K and pressures of 190 GPa in our main text. In this supplementary material, we include some of the details on pressure measurements, analyses of low temperature x-ray diffraction, and analyses of electrical conductivity data.

Samples were prepared using a multi-step process with various piston cylinder-type diamond anvil cells [1], Compound gaskets consisting of a tungsten outer annulus and a cubic boron nitride (cBN) insert were employed to encapsulate the sample at megabar pressures while isolating the electrical leads. Samples synthesized using in-situ diffraction and laser heating were then loaded into a cryostat for conductivity measurements [2].

The samples used for the electrical conductivity measurements and in low temperature x-ray diffraction are shown in Table S1. The synthesis pressures listed are the pressures before based on the diamond Raman measurements [3] and corroborated with Pt and La equations of

state [4,5]. The cell volumes listed are the volume per formula unit and are based on the position of the (111) diffraction peak of $\text{LaH}_{10\pm x}$ (Fm-3m). The (110) and (024) diffraction peaks of La were used to constrain the cell volume of its *hr24* (R-3m) phase.

The normalized resistance $R(T)-R_c(T)/R(300 \text{ K})-R_c(T)$, where R_c is the estimated contact resistance as a function of temperature and R_{300} is the ambient temperature resistance of $\text{LaH}_{10\pm x}$ along with that of pure La measured with a pseudo-four probe technique are shown in Fig. S1. The measurements were made using a pseudo four-point geometry and therefore the observed resistance is a sum of the sample resistance and the contact resistance [6]. Figure S2 shows an example of steps used in correcting for the contact resistance and obtaining the relative variation of the sample resistance as a function of temperature.

The results of the low-temperature x-ray diffraction results are shown in Fig. S3 and S4. Due to the large ‘footprint’ of the cryostat (a flow type L-N_2 cryostat equipped with sapphire windows), a beam defining, collimating pinhole could not be placed close to the sample and correspondingly, a larger incident beam interrogated several parts of the sample at the same time. Further, due to differential contraction of several components in the cryostat, it is very difficult to interrogate the exact same part of the sample at different temperatures. We therefore obtained several diffraction patterns in a $50 \times 50 \mu\text{m}$ grid (in $10 \mu\text{m}$ steps) and analyzed all of them. The data was fitted with several diffraction peaks comprising the sample, the pressure marker and cryostat window. This was a preferred method for extracting the d-spacings of Pt and $\text{LaH}_{10\pm x}$ since any profile refinement would not be able to account for pressure distribution as well as sample inhomogeneity. Apart from the stronger diffraction peaks ascribed to the cryostat exit window, we see no evidence for any new diffraction that would indicate a structural transition in cubic $\text{LaH}_{10\pm x}$ in the $80 - 300 \text{ K}$ temperature interval at 185 GPa .

Table S1: Samples used for electrical conductivity and low-temperature x-ray diffraction measurements.

Sample	Synthesis Pressure	Cell Volume	Experimental Details
A	$185(\pm 5) \text{ GPa}$	$32.0(2) \text{ \AA}^3$	Four probe electrical conductivity
B	$188(\pm 5) \text{ GPa}$	$31.1(2) \text{ \AA}^3$	Pseudo-four probe conductivity
C	$175(\pm 5) \text{ GPa}$	$29.8(2) \text{ \AA}^3$	Pseudo-four probe conductivity
D	$180(\pm 5) \text{ GPa}$	$14.5(2) \text{ \AA}^3$	Four probe electrical conductivity
E	$182(\pm 5) \text{ GPa}$	$27.8(2) \text{ \AA}^3$	Low temperature x-ray diffraction

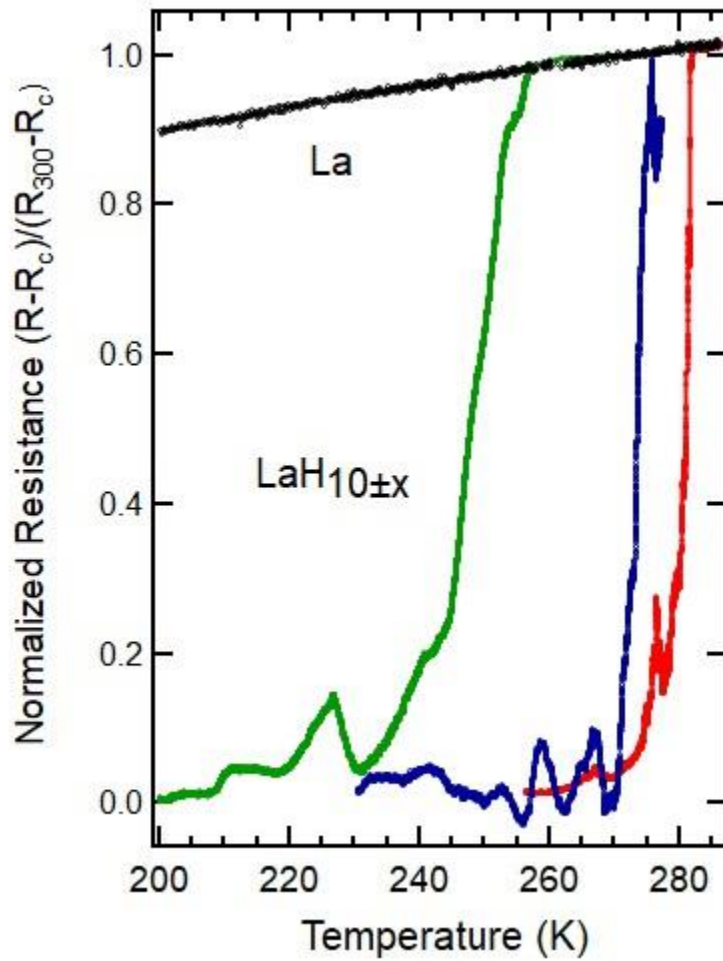


Figure S1. The normalized resistance $(R(T) - R_c(T)) / (R(300 \text{ K}) - R_c(T))$ of $\text{LaH}_{10\pm x}$ (sample B) along with that of pure La (sample D) measured with a pseudo-four probe technique. The pressure measured at room temperature with the diamond Raman gauge [3] increased gradually with every cooling and warming cycle, as determined from measurements performed after the sample was extracted from the cryostat; i.e., 190 GPa (green), 195 GPa (blue) and 202 GPa (red) for the three warming and cooling cycles. A correction for a linear contact resistance was applied since this was a three-point measurement. Although the apparent increase in T_c with pressure increase contradicts both theory [7] and our four-probe measurement (sample A; Fig. 3), the behavior could actually represent changes in sample connectivity and stoichiometry similar to that reported in H_3S [8].

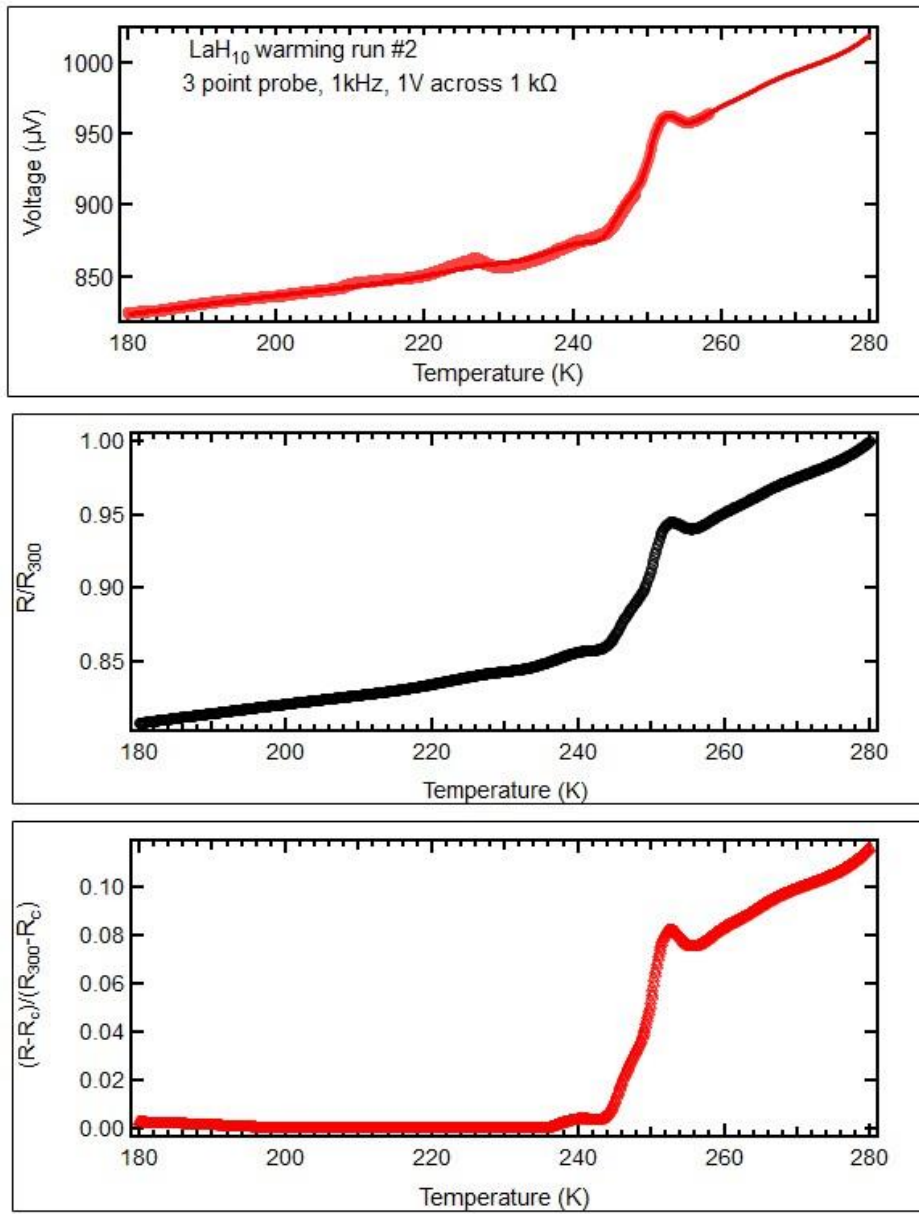


Figure S2. Selected resistance data obtained from the pseudo-four probe measurement of $\text{LaH}_{10\pm x}$ during a warming cycle from 150 K. The raw data shown in the top panel was normalized to the ambient resistance value (in this case, an extrapolated value) to obtain the relative resistance (R/R_{300}). As is evident from the second panel, this ratio drops at about 250 K and shows a linear decrease thereafter. We assume that the linear resistance below this drop signifies a residual contact resistance which is subtracted out of the whole curve to produce the curve in the lowest panel. This would therefore correspond nominally to a relative resistance corrected for a contact resistance. The same procedure was applied to several other measurements made on this sample (B) as displayed in Fig. S1.

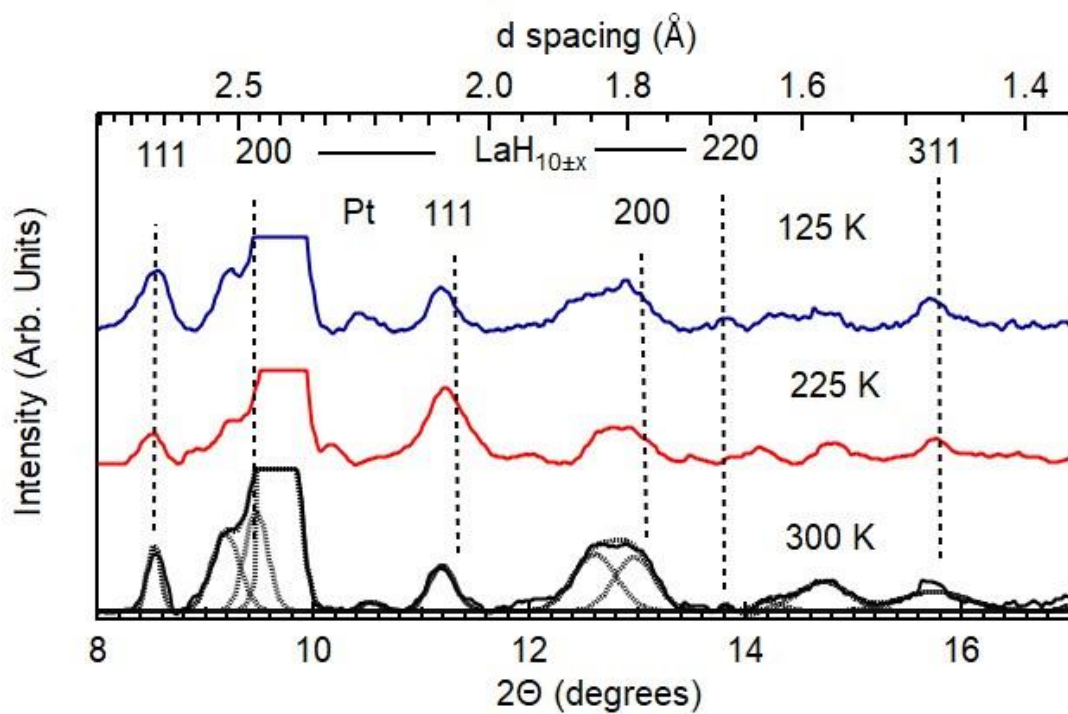


Figure S3: Powder x-ray diffraction patterns obtained during cooling of $\text{LaH}_{10\pm x}$ (sample E) after synthesis at 182 GPa. The d-spacings of the relevant diffraction peaks (listed in the upper two panels of the figure), were obtained from a fit like that shown for the 300 K pattern.

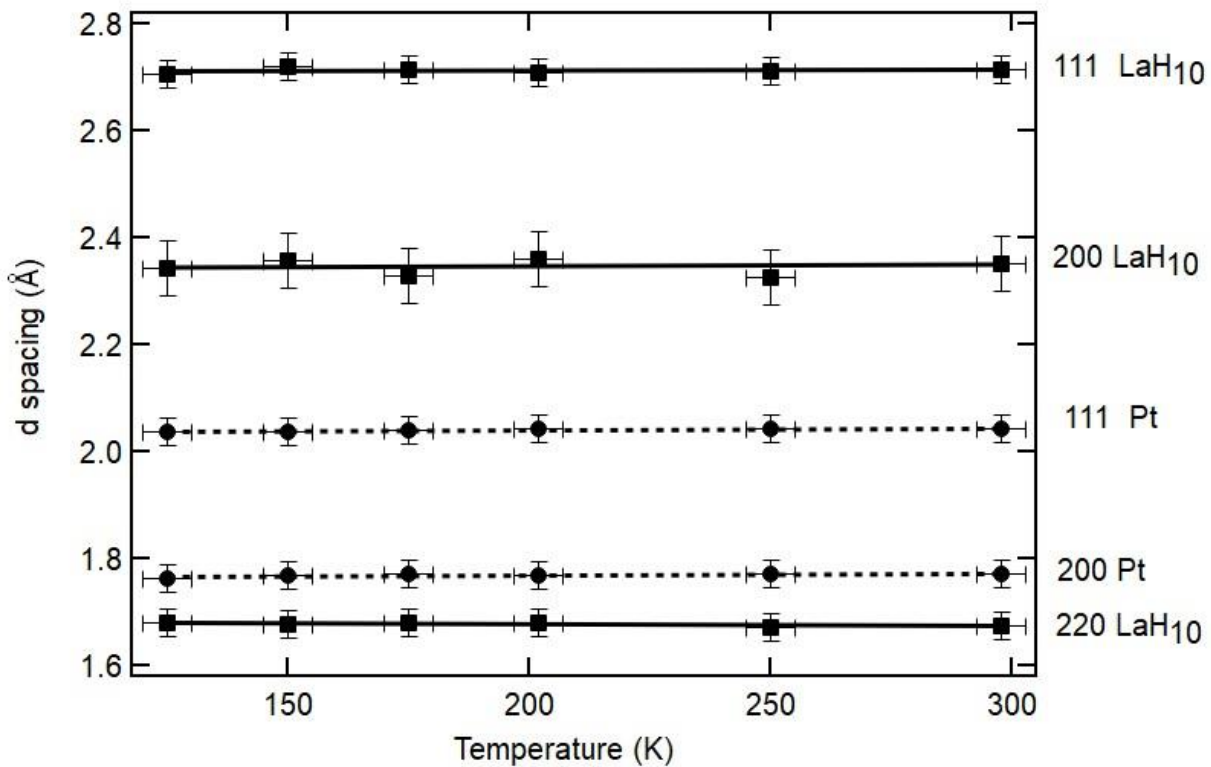


Figure S4: Observed d-spacings of $\text{LaH}_{10\pm x}$ and Pt as a function of temperature at 185 GPa taken from analysis of patterns such as those shown in Fig. S3. The error bars for the 200 line of $\text{LaH}_{10\pm x}$ are larger because they were extracted from a fit to three overlapping diffraction peaks (see Fig. S3). The parameters of the accompanying, stronger diffraction peaks arising from the cryostat windows were fixed in the refinement. Coupled with this is also the effect of pressure broadening which manifests itself in at least two diffraction peaks corresponding to two pressures that are offset by at least 20-30 GPa. We choose the highest-pressure peak (although it could be smaller in intensity) and display this position in the figure above with the peak width as the error bar. The error in pressure is determined from the width and indeterminacy of the Pt diffraction peaks. The lines show that there is neither a large pressure drift nor change in the P - V dependence of $\text{LaH}_{10\pm x}$ in this temperature range. In general, our experience with the stainless steel (SS) long piston-cylinder cells equipped with SS spring washers has been that the pressure increases on cooling (at least in the first cycle) by about 10-20 GPa due to changes in washer dimensions and thereby the load. In this experiment, we used non-magnetic cells and Be-Cu spring washers [1], which show smaller pressure drifts due to changes in load.

References:

[1] A. G. Gavriluk, A. A. Mironovich, V. V. Struzhkin, Miniature diamond anvil cell for broad range of high pressure measurements, *Rev. Sci. Instr.* **80**, 043906 (2009).

[2] J. Y. Zhao, W. Bi, S. Sinogeikin, M. Y. Hu, E. E. Alp, X. C. Wang, C. Q. Jin, and J. F. Lin, A compact membrane-driven diamond anvil cell and cryostat system for nuclear resonant scattering at high pressure and low temperature, *Rev. Sci. Instr.* **88**, 125109 (2017)

[3] Y. Akawama and H. Kawamura, “High-pressure Raman spectroscopy of diamond anvils to 250GPa: Method for pressure determination in the multimegabar pressure range”, *J. Appl. Phys.* **96**, 3748-3751 (2004).

[4] A. Dewaele, P. Loubeyre and M. Mezouar, Equations of state of six metals above 94 GPa, *Phys. Rev. B* **70**, 094112 (2004).

[5] Z. M. Geballe, *et al.*, Synthesis and stability of lanthanum superhydrides, *Angew. Chem. Inter. Ed.* **57**, 688-692 (2018).

[6] M. Eremets and I. Trojan, Conductive dense hydrogen, *Nature Mater.* **10**, 927–931 (2011).

[7] H. Liu, I. I. Naumov, R. Hoffmann, N. W. Ashcroft and R. J. Hemley, Potential high- T_c superconducting lanthanum and yttrium hydrides at high pressure, *Proc. Natl. Acad. Sci. USA* **114**, 6990-6995 (2017).

[8] [A.P. Drozdov](#), [M. I. Eremets](#), [I. A. Troyan](#), [V. Ksenofontov](#), [S. I. Shylin](#), Conventional superconductivity at 203 K at high pressures, *arXiv:1506.08190* (2015)